ASR GELS AND THEIR CRYSTALLINE PHASES IN CONCRETE – UNIVERSAL PRODUCTS IN ALKALI-SILICA, ALKALI-SILICATE AND ALKALI-CARBONATE REACTIONS

Tetsuya Katayama

Kawasaki Geological Engineering Co. Ltd., Tokyo, Japan

Abstract

Reaction products of AAR, gels and crystalline rosettes, have similar compositions, irrespective of the type of AAR and aggregate, i.e. early- or late-expansive ASR, alkali-silicate or alkali-carbonate reaction. The root cause of expansion is ASR of silica minerals. Alkali-rich gels crystallize in continuous cation distributions of tetrahedral (8.0-8.5) and octahedral sites (4.0-5.5, O=20) between cryptophyllite and rhodesite, particularly suggestive of a solid solution of mountainite-shlykovite. XRD analysis gave no single known mineral peaks, but those of mountainite -shlykovite plus either fedorite or reyerite, indicative of a mixture or a mixed layer between these. ASR gels had $SiO_2/(Na_2O+K_2O)$ from 5-6 in andesite to 8 in rhyolite. They were unstable during SEM observation and long-term storage, and liberated high-alkali silicate sol (<3), leaving silica-rich host gel (>8). This explains why two types of ASR sol/gel, i.e. fluid alkali-rich and viscous silica-rich, coexist within same concretes: they form in equilibrium with relative humidity in concrete. Expansion is likely due to the swelling pressure of water by ASR gel.

Keywords: ASR gel, alkali-carbonate reaction, alkali-silicate reaction, EDS analysis, rosette.

1 INTRODUCTION

In a study of ASR products, which range from low-Ca through high-Ca ASR gel to CSH gel on the [Ca/Si]-[Ca]/[Na+K]) diagram, Katayama in 2010 [1] predicted the missing links on the tie line of natural minerals with [Ca/Si]=1/4 and 1/5 at [Ca]/[Na+K]=1. Subsequently, Pekov et al. [2] described new minerals shlykovite (1/4, 1) and cryptophyllite (1/4, 1/2) from the alkaline complex in Russia, the former meeting this condition. Because Na-K-Ca-silicate hydrate minerals have been described separately from different parts of the world, no systematic interpretation has yet been done with respect to AAR products. Hence, a review was made of author's analytical data of ASR gels and rosettes in concretes to refine and reinterpret them (Table 1)[3].

2 MATERIALS AND METHODS

Samples came from 16 AAR-affected concrete structures, including cases of 6 ASR in Japan, 3 ASR in New Brunswick, 4 ASR in Quebec (1 from Dr. B Fournier), 1 ASR in Norway from Dr. M Haugen, 1 typical ACR in Ontario from Mr. CA Rogers, 1 highly weathered ASR from Newfoundland, plus 2 ASR-concrete prisms from Mr. DJ Bragg with Newfoundland aggregate, and 1 mortar bar of alkali-silicate reaction with Nova Scotia aggregate from Dr. PE Grattan-Bellew. Polished thin sections (20-25mm by 30-35mm, thickness 15μm) were analyzed for reaction products by the author with EDS (JEOL JSM 5310LV/JED2140, 15kV, 0.08-0.12nA) in the past 10 years, or with WDS 22 years ago (JEOL JCMA733, 15kV, 10nA), using ZAF correction and the same standard. Details of sample preparation and precision of EDS analysis were given in [1]. Compositions of rosette crystals were compared with published analytical data of natural Na-K-Ca-silicate and Ca-silicate hydrate minerals. For concretes from New Brunswick, Canada, data of micro-XRD analysis of extracted void-filling products (2-3mm) (Rigaku PSPC- MDG, CuKα, 6-60º2θ, 60KV, 200mA, beam diameter 100μm, step size 0.08º2θ) [4] were re-interpreted [3] in view of the recent findings of shlykovite and cryptophyllite.

3 RESULTS

3.1 Compositions of natural alkali-calcium silicate hydrate minerals

* Correspondence to: katayamat@kge.co.jp

Rosette crystals in ASR have natural counterparts of alkali-bearing calcium silicate hydrate minerals: cryptophyllite $(K,Na)_4Ca_2Si_8O_{20}\cdot 10H_2O$, mountainite $Ca_2Na_2KSi_8O_{19.5}6.5H_2O$, fedorite $K_{0.5}Na_2Ca_2Si_8$, $O_{19.25}\cdot 4H_2O$ ($OH=0.5O+0.5H_2O$), shlykovite $(K,Na)_2Ca_2Si_8O_{19}7H_2O$ and rhodesite $KCa_2Si_8O_{18.5}6.5H_2O$ according to the latest references (Table1). Published compositions were recalculated for cation numbers of tetrahedral versus octahedral site including the interlayer position at fixed O=20 [3]. They constitute 1) the Na-K-Ca-silicate hydrate tie-line between cryptophyllite and rhodesite, and 2) the Ca-silicate hydrate tie-line extending from the low Ca/Si group (<1.5) on Figure 1a (tobermorite, clinotobermorite, gyrolite, okenite, reyerite, zeophyllie and apophyllite) to the high Ca/Si group outranged here (hillebrandite, jennite, foshallasite and afwillite). On the [Ca/Si]-[Ca]/[Na+K] diagram, they present a compositional trend line (Figure 1b) resembling typical ASR gels in concrete (Figure 1c) which show a sigmoidal curve on the alkali concentration-distance diagram (Figure 5a) suggestive of a diffusion process between alkalis and calcium at the boundary of the aggregate.

3.2 Compositions of rosette crystals and cation site diagram

The compositions of rosette crystals found in ASR and ACR-affected concretes were plotted on the cation site diagram at normalized O=20, tentatively assigning cations to the tetrahedral (Si, Al, S) and octahedral (Ca, Mg, Fe, Ti, Mn) plus interlayer sites (Ca, Na, K)[3]. They lie on the similar trend lines passing mountainite and shlykovite mostly within a triangle of cryptophyllite, reyerite and rhodesite, irrespective of *early-expansive* (Figure 2a) or *late-expansive* ASR in Japan (Figures 2b,c), ASR of Norwegian (Figure 2d) or Canadian limestones (Figure 2e), typical ACR in Ontario (Figure 2f) or ASR in New Brunswick associated Ca-rich gel (Figure 2g), with or without freeze-thaw cycles after NaOH immersion in concrete prisms made with Newfoundland aggregate (Figure 2h). In weathered concretes, however, compositional trend lines of rosette crystals tend to be gently sloped, deviating from the trend line of Na-K-Ca-silicate hydrates towards the Ca-silicate hydrates (Figures 2 g,h). This is suggestive of the leaching of alkalis from the rosettes and introduction of calcium, as shown by the scattered data in Figure 5b [3,5].

Rosette crystals were recalculated for cation numbers with corresponding oxygen numbers (20 to 18.5) and selected data were shown in Table 2. With this condition, ideal compositions of these minerals had a total of octahedral and interlayer cations, decreasing from cryptophyllite (6.0), through mountainite (5.0), fedorite (4.5) and shlykovite (4.0) to rhodesite (3.0). It displays a good stoichiometry with mountainite and shlykovite irrespective of the type of AAR, with a transition to cryptophyllite and rhodesite. The analytical sum totals of the rosettes were about 20% smaller than their natural counterparts. This is likely due to thin flaky crystals (thickness 0.2-1μm, length 5-10μm) with a porous texture with wedge-shaped morphology that penetrates or disperses the electron beam (Figure 3), whereas published data of natural minerals are based on larger crystals (thickness 20-50μm, length >200μm) enough to apply diffused electron beam (e.g. >10μm) [2].

3.3 XRD analysis of rosette crystals

The Na-K-Ca-silicate hydrate minerals, natural analogues of rosette crystals, have similar structures of tetrahedral-octahedral sheets, giving similar d-spacings at higher diffraction angles, but give different basal reflections due to varied interlayer spaces and hydration state (Table 3). Air void-filling rosettes in New Brunswick concrete (B-90B), with average composition $(Na_{0.44},K_{0.56})_2O\cdot 1.96CaO\cdot 5.77SiO_2\cdot nH_2O$ [1,3], had coordinated atoms of octahedral=5.43, tetrahedral=7.96 at O=20 (Figure 2g), closer to mountainite (octa= 5.13, tetra=8.21) than shlykovite (octa=4.21, tetra=8.42), while they are indistinguishable by XRD giving a 13Å peak and other similar peaks (Table 3). Massive to reticular gel (P-57C) had a 11.9Å peak close to fedorite. Well-developed void-filing rosette (T-70A) gave peaks of mountainite-shlykovite, along with 9.7Å peak resembling reyerite. This suggests that these crystalline products are a mixture of several phases, or a mixed layer sheet silicate like clay minerals, but the latter needs a check of super-lattice reflection.

3.4 Spontaneous separation of ASR sol/gel from ASR gel during storage

ASR gel is vulnerable to environmental changes of relative humidity and temperature. Higher temperature and/or vacuum, introduced by electron beam in EDS analysis and storage, may liberate absorbed water dissolving certain amount of water-soluble alkali. To investigate this effect, a $[CaO]/[Na_2O+K_2O+CaO]$-$[SiO_2]/[Na_2O+K_2O+CaO]$ diagram was proposed, assuming substitution of $(Na, K)_2O=CaO$ [3].

In this condition, crystalline rosettes were found relatively stable compared with amorphous gels. During 1 year of storage, rosettes had liberated moisture as liquid spots onto the surface of thin section (Figures 4a,b, box culvert, andesite, 22 years), but only a small amount of Na ion was leached corresponding to a slight compositional change from mountainite to shlykovite (Ma1 to Ma2, Table2). By contrast, alkali-rich gel was very active and unstable (box girder, andesite, 26 years). In this deteriorated concrete, rosettes were not found indicating that the

cracking was caused by ASR gel. On the polished thin section, ASR gel had separated liquid spots which were noticeable under reflected light. 9 years later, these blots were cleaned up by re-polishing the thin section for EDS analysis for the second time. It was found that the original single compositional line (Figure 4c) was split into two lines, of which low-Ca and high-alkali line (Ca ratio <0.4) shifting about 4 to the siliceous side on the abscissa (Figure 4d).

Finally, compositions of the separated liquid spots were analyzed directly by EDS analysis (Figures 4e,f). In this case, a reacted rhyolite glass (gate pier, 39 years) had produced ASR gel and popped out 1 week after coring (Figure 4e). This gel separated alkali-silica sol after 1 year of storage, leaving siliceous host ASR gel (Figure 4f). Thus, the $[SiO_2]/[Na_2O+K_2O]$ ratios of primary ASR gel, extrapolated to CaO=0, range from 5 for andesites (Figures 4a,c) to 8 for glassy rhyolite, the latter further split into 3 for separated sol and 10 for remaining gel (Figures 4e,f). The liquid separation observed in this study well explains the reason why ASR gel presents bimodal distribution, i.e. less-siliceous mobile ASR gel and siliceous viscose ASR gel (Figure.4g).

3.5 Alkali-silicate reaction (ASLR)

The terminology of alkali-silicate reaction was abandoned in Canada nearly two decades ago, and has been assigned to the category of alkali-silica reaction that occurs with various varieties of quartz (CSA-A23.1-94). However, on this revision, the most important aspect of this reaction proposed by the original authors Gillott et al. [6] has not yet been clarified. They claimed that phyllosilicate, vermiculite-like mineral pseudomorphic after biotite, alters to an expandable clay mineral to exfoliate in concrete, and that silicate gel is liberated from the interlayer materials of the phyllosilicate. Hence, an accelerated mortar bar (CSA A23A-25A), made using typical alkali-silicate reactive greywacke-argillite from Nova Scotia (sandstone-mudstone undergoing lower grade metamorphism) and produced deleterious expansion (0.34% at 14 days), was examined by SEM-EDS for reaction between minute phyllosilicate flakes (10-20 μm) and cement paste, and other reaction products [3].

Under SEM, microcrystalline quartz reacted to form cracks filled with ASR gel and crystalline rosettes. On the [Ca/Si]-[Ca]/[Na+K] diagram, both gel and rosettes showed a compositional trend line of typical ASR products (Figure 5c). Similar Japanese aggregate of slightly higher grade metamorphism produced damage to field concrete, in which microcrystalline quartz had partly converted to ASR gel and rosettes without digesting flakes of biotite and muscovite (Figure 3g). None of the phyllosilicates biotite $K_2(Mg,Fe)_6\,Al_2Si_6\,O_{20}(OH)_4$ $(=O_{22}2H_2O)$, muscovite $K_2Al_4(Al_2Si_6)\,O_{20}\,(OH)_4$ $(=O_{22}\,H_2O)$ or chlorite $(Mg,Fe)_{3\cdot}\,(Mg,Fe,Al)_{3\cdot}\,(Al,Si)_aO_{10\cdot}(OH)_8$ $(=O_{14}4H_2O)$ contacting ASR gel or rosettes, presented evidence of reaction or exfoliation (Figure 3f, Table 4)[3]. This means that the proposed mechanism for alkali-silicate reaction [6] is impossible.

Muscovites had normal interlayer cation numbers (K=2.0) without evidence of releasing potassium into cement paste, and was distinguished from illite: $(K,H_3O)_2(Al,Mg,Fe)_4\,(Si,Al)_8O_{20}\,[(OH)_4,\,2(H_2O)]$ $(=O_{22}4H_2O)$ with an interlayer vacancy (K<1.7). Biotite presented vacancies in both octahedral and interlayer sites suggestive of leaching of K, Mg and Fe, but it is within a range of natural rock weathering in the field, and not suggestive of the formation of hydrobiotite or vermiculite. Microcrystalline quartz was always responsible for the expansion cracks filled with ASR gel, hence ASLR of Canadian aggregate is a late-expansive ASR.

4 DISCUSSION

Most of the data in this paper came from analyses performed during 2009-2010: Figures 2a (Ma1, Japan, 2009), 2b (Mi, Japan, 2009), 2c (Oh, Fu, Japan, 2004), 2d (Norway, 2009), 2e (Quebec, 2006), 2f (Ontario, mainly 2003), 2h (Newfoundland, 2003); Figures 4a (Ma1, 2009), 4b (Ma2, Japan, 2010), 4c (Ji, 2001), 4d (Ji, Japan, 2010), 4e (To, Japan, 2009), 4f (To, Japan, 2010); plus Table 2 (NS, Canada, 2010; Ms4, Japan, 2007) and Table 4 (NS; Hy, Japan 2010). Only data in Figure 2g (NB, Canada, 1988) were obtained by WDS using the same mineral standards. Since 1998, the same SEM-EDS has been used under essentially same operating condition with the same standards and thin sectioning process, as noted in [1]. Hence all analyses presented here can be compared directly.

The observed continuous range of composition of rosette crystals (Figure 2a, Ma Japan) most probably inherited from original ASR gels with a compositional gradient that had formed by diffusion between alkali ions in ASR gels and calcium ions in cement paste (Figures 1c, 5a). Their natural counterpart crystalline phases have been described as independent minerals, not as a solid-solution [2, 17-24], because different oxygen numbers were applied to accommodate their small compositional variations. They need a systematic comparative study, as in [5].

It has generally been accepted that expansion mechanism of ASR involves two steps of reaction, i.e. 1) formation of alkali-silica gel or related precursor phase from silica minerals and alkalis, producing a considerable volume increase [1], and 2) swelling of gel by water adsorption [3, 15] or other mechanism. In this chapter, the second process will be discussed in relation with the occurrence of rosette crystals and gel products in concrete.

4.1 Does crystallization of rosettes from ASR gel exert expansion pressure?

What does crystallization of rosettes affect ? They crystallize from ASR gel [7], keeping the same cation ratio as the host gel vein (e.g. Fig.3a)[8]. This can be written as Eq.(1), taking mountainite as a rosette phase.

Mountainite gel → Mountainite crystal + dehydration

$$Na_2O{\cdot}0.5K_2O{\cdot}2CaO{\cdot}8SiO_2{\cdot}nH_2O \rightarrow Na_2O{\cdot}0.5K_2O{\cdot}2CaO{\cdot}8SiO_2{\cdot}6.5H_2O + (n\text{-}6.5)H_2O \qquad \text{Eq.(1)}$$

Because the density of this gel is unknown, this process is approximated by the simple sodium-silicate gel and one of its crystalline phases kanemite out of crystalline products (e.g. kanemite $Na_2O{\cdot}4SiO_2{\cdot}7H_2O$ 1.93, revdite $Na_2O{\cdot}2SiO_2{\cdot}5H_2O$ 1.94; shlykovite $K_2O{\cdot}2CaO{\cdot}8SiO_2{\cdot}7H_2O$ 2.21; mountainite 2.36). According to Vivian's data [9], viscoelastic sodium silicate gels capable of generating the expansive force under loading (with approximate $[Na_2O]/[SiO_2]$ of 1/5, although not 1/4) have a water content ranging between 40% and 65% (Figure 5f), with the maximum density (1.4) corresponding to the minimum water content (40%). The Eq.(2) means that the crystallization of this gel into kanemite, for example, will reduce about 40% of the molar volume, i.e. contraction interspaces appear between crystals without producing crystallization pressure. Similar contraction will also occur in the Ca-bearing gel that forms rosettes of mountainite or shlykovite in Eq.(1) (e.g. Figure 3a).

ASR gel (H_2O=40 wt%) → kanemite + dehydration

$$Na_2O{\cdot}4SiO_2{\cdot}11H_2O \rightarrow Na_2O{\cdot}4SiO_2{\cdot}7H_2O + 4H_2O \qquad \text{Eq.(2)}$$

Molar volume 500/1.4=357 428/1.93=222
Volume decrease (222-357)x100/357 = -38%

4.2 Do rosette crystals precipitate from supersaturated solution producing crystallization pressure?

Another type of crystallization of a new phase has often been noted from supersaturated solutions in cement chemistry, in which crystallization pressure is calculated from the degree of supersaturation (DS) of interstitial water relative to the phase in question. Correns and Steinborn [10] gave a rough definition for C/Cs in solute concentrations (Eq.3), instead of using the activities of the solution. Even not accurate, this equation has been used conveniently for the precipitation of salts from aqueous solution. For example, with a DS of 5 at 25 ºC, crystallization pressure of mountainite 1/2 $[Na_2O{\cdot}0.5K_2O{\cdot}2CaO{\cdot}8SiO_2{\cdot}6.5H_2O]$ could be of the order of 200 atm, which exceeds that of mirabilite $Na_2SO_4{\cdot}10H_2O$ (182 atm) and ettringite (56 atm).

However, according to SEM observations, rosette crystals in ASR-affected concretes occur as a secondary growth within the precursor ASR gel, and not a direct precipitate from aqueous solution within open spaces such as air voids or open cracks in concrete. Thus the mechanism of the crystallization pressure does not apply to the rosette crystals in ASR, and hence other expansion mechanism should be searched for.

$$\Delta P=(RT/Vm) \times \ln C/Cs \qquad \text{Eq.(3)}$$

Where R: Gas constant, T: temperature (K), Vm: molar volume, C/Cs: degree of supersaturation. For mountainite, Vm=173.50 $\times 10^{-3}$, $\Delta P = (8.206\times10^{-2} \times 298/173.50 \times 10^{-3}) \times 1.609 = 227$ atm.
For shlykovite $KCa[Si_4O_9(OH)]{\cdot}3H_2O = 1/2[K_2O{\cdot}2CaO{\cdot}8SiO_2{\cdot}7H_2O]$, Vm=183.94 $\times 10^{-3}$, ΔP =214 atm.

4.3 Hydrostatic swelling pressure of ASR gel

Two types of ASR gel have been known: 1) highly fluid alkali-rich ASR sol exuded onto concrete surface [11] with $SiO_2/(Na_2O+K_2O)$ ratio of 3-4 (CaO: virgin gel 0%, older gel up to 12%), and 2) siliceous viscous ASR gel in concrete [12] with that ratio up to 8. This aspect is well illustrated on the proposed diagram $[CaO]/[Na_2O+K_2O+CaO]$-$[SiO_2]/[Na_2O+K_2O+CaO]$ (Figure 4g). Experimental data [13] indicates that an equilibrated pair of liquid and gel has a maximum osmotic pressure at $[SiO_2]/[Na_2O]$=4-5 (Figure 4h). Thus, the observed separation of alkali-rich sol from ASR gel corresponds to this pair, which means ASR gel releases alkali-rich sol reflecting the relative humidity (RH) in concrete. Published data of soluble alkali silicates [14], extrapolated here to SiO_2/Na_2O=5 (wt%) and 10^4 poises (Figure 5d), shows that their viscosity decreases drastically with a small increase of water. For ASR gel to develop expansive force, viscosity must have a pessimum range so as not to penetrate cement paste but to keep suitable elasticity, say 15 to the order of 10^4 poises [15]. Its upper limit may be higher in concrete, > 10^5 poises under loading, because gel viscosity might drop by pressure solution.

Hydrostatic swelling pressure by water vapor adsorption of ASR gel can be calculated from the relationship between relative humidity RH and molar volume of water, Eq (4), given by Krogh [3, 15]:

$$\Delta P = (RT/V) \times \ln(1/RH) \qquad \text{Eq.(4)}$$

where R: Gas constant, T: temperature (K), V: molar volume of water, RH: relative humidity. Thus, ASR gel with $SiO_2/Na_2O=3$ with extrapolated viscosity (i.e.10^5 poises) will have 50% water (Figure 5d), which should have equilibrium RH at 93% (Figure 5e). ASR gel formed or stable at this equilibrium RH will produce a pressure of about 100kg/cm^2 by adsorbing moisture, which is sufficient to crack concrete:

$$\Delta P=(RT/V)\times \ln(1/RH) =(8.206\times10^{-2}\times298/18 \times 10^{-3}) \times \ln (1/0.93) =1358.55\times0.073= 99 \text{ atm}$$

It has been noted, however, that ASR gel has a pessimum RH (ca 90%) with respect to expansion, as Nilsson [16] and Jensen [7] pointed out, because gel dried at lower RH is too rigid to expand whereas gel formed at appropriate RH produces larger pressure, but gel in contact with 100% humidity or water dissolves into water, thus producing smaller pressure. For instance, on the inner wall of a concrete canal (Figure 5g) with a permanent water-flow, ASR sol from andesite aggregate dissolves into water before polymerizing into ASR gel, and produces no expansion cracks, whereas subaerial portion subject to repeated drying/wetting develops pronounced expansion cracks rich in ASR gel. Several cracked structures contain only ASR gel without rosette crystals (typically, Ji bridge, Figs.4c,d). Likewise, amorphous ASR gel produces explosive pop-outs on the concrete surface (Figures 4e,f). It is therefore reasonable to conclude that the expansion of concrete is caused by ASR gel, and not by rosette crystals.

5 CONCLUSIONS

- ASR gel and crystalline rosettes are universal products of AAR, i.e. early- and late-expansive ASR, ACR and alkali-silicate reaction. All the expansion mechanisms of AAR are now attributable to ASR of silica minerals. Alkali-rich ASR gels crystallize into rosettes on the tie line of cryptophyllite-rhodesite, possibly forming a solid solution between mountainite and shlykovite, or a mixed layer of wider range which needs further study.
- The formation of rosette crystals from ASR gel does not produce a volume increase or crystallization pressure. Micro-environmental changes in concrete (relative humidity) cause minor leaching of Na from rosettes modifying mountainite to shlykovite by composition, as well as liberation of alkali-rich ASR sol from ASR gel, leaving siliceous ASR gel. Hydrostatic pressure of ASR gel due to water adsorption is responsible for expansion.

6 REFERENCES

[1] Katayama, T (2010): The so-called alkali-carbonate reaction (ACR)-Its mineralogical and geochemical details, with special reference to ASR. Cement and Concrete Research (40), 643-675.

[2] Pekov, IV, Zubkova, NV, Filinchuk, YE, Chukanov, NV, Zadov, AE, Pushcharovsky, DY and Gobechiya, ER (2010): Shlykovite $KCa[Si_4O_9(OH)]\cdot3H_2O$ and cryptophyllite $K_2Ca[Si_4O_{10}]\cdot5H_2O$, new mineral species from the Khibiny alkaline pluton, Kola peninsula, Russia. Geology of Ore Deposit (52), 767-777.

[3] Katayama, T (2012a): Petrographic study of alkali-aggregate reactions in concrete. Doctoral thesis (Science), Department of Earth and Planetary Science, Graduate School of Science, The University of Tokyo. 168p.

[4] Katayama,T and Futagawa,T (1989): Alkali-aggregate reaction in New Brunswick, eastern Canada -Petrograpghic diagnosis of the deterioration. Proceedings, 8th International Conference on Alkali-Aggregate Reaction in Concrete. Kyoto, Japan. 531-536.

[5] Katayama, T (2012b): Late-expansive ASR in a 30-year old PC structure in Eastern Japan. Proceedings, 14th International Conference on Alkali-Aggregate Reaction (ICAAR), this conference, Austin, Texas, USA.

[6] Gillott, JE., Duncan, MAG., and Swenson, EG., (1973): Alkali-aggregate reaction in Nova Scotia, IV Character of the reaction. Cement and Concrete Research, Vol.3, 521-535.

[7] Jensen, V. (1993): Alkali aggregate reaction in southern Norway. Doctor Technicae thesis, The Norwegian Institute of Technology, University of Trondheim. 262p

[8] Katayama, T, Sarai, Y, Higashi, Y, and Honma, A (2004): Late-expansive alkali-silica reaction in the Ohnyu and Furikusa headwork structures, central Japan. Proceedings, 12th International Conference on Alkali-Aggregate reaction in Concrete (ICAAR), Beijing, China, 1086-1094.

[9] Vivian, HE (1950): The reaction product of alkalies and opal. Studies in Cement-Aggregate Reaction. Part XV. CSIRO Melbourne, Australia. Bulletin 256, 60-81.

[10] Correns, CW and Stinborn, W (1939): Experimente zur Messung und Erklung der sogenannte Kristalisationskraft. Zeitschrift für Kristallographie (101), 117

[11] Idorn, GM (1961): Studies of disintegrated concrete, Part 1 progress report N2, The Danish National Institute of Building Research and the Academy of Technical Sciences, Committee on alkali reactions in concrete, Copenhagen, 77p.

[12] Knudsen, T and Thaulow, N (1975): Quantitative microanalyses of alkali-silica gel in concrete. Cement and Concrete Research (5), 443-454.

[13] Glasser, LSD and Kataoka, N (1981): The chemistry of 'alkali-aggregate' reaction. Cement and Concrete

Research (11), 1-19.
[14] Vail, JG (1952): Soluble silicates, their properties and uses. Volume 1: Chemistry. Reinhold Publishing Corporation, New York. (Fig.3.33. p.82). 357p.
[15] Krogh, K (1975): Examination of synthetic alkali-silica gels, Proceedings, Symposium on Alkali-Aggregate Reaction, Reykjavik, Iceland. 131-163.
[16] Nilsson, LO (1983): Moisture effects on the alkali-silica reaction. Proceedings, 6th International Congress on the Alkali-Silica Reaction (ICAAR), Copenhagen, Denmark, 201-208.
[17] Zubkova, NV, Pekov, IV, Pushcharovsky, Y and Chukanov, NV (2009): The crystal structure and refined formula of mountainite, $KNa_2Ca_2[Si_8O_{19}(OH)]\cdot 6H_2O$. Zeitschrift für Kristallographie (224), 389-396.
[18] Mineralogy database: *http//webmineral.com*mountainite, rhodesite, ryerite, fedorite.
[19] Handbook of mineralogy: *http//www.handbookofmineralogy.org* mountainite, rhodesite.
[20] Gard, JA and Taylor, HFW (1957): An investigation of two minerals: rhodesite and mountainite. Mineralogical Magazine (31), 611-623.
[21] Mitchell, RH and Burns, PC (2001): The structure of fedorite: A re-appraisal. The Canadian Mineralogist (39),769-777.
[22] Blackburn,WH and Deennen, WH (1997): Encyclopedia of Mineral Names. Mineralogical Assocation of Canada. Special Publication 1.
[23] Hesse, FK and Liebau, F (1992): Crystal structure of rhodesite, $HK_{1-x}Na_{x+2y},Ca_{2-y}\{IB,3,2^2\infty\}\ [Si_8O_{19}]\cdot(6-z)H_2O$, from three localities and its relation to other silicates with dreier double layers. Zeitschrift für Kristallographie (199), 25-48.
[24] Mountain, ED (1957): Rhodesite, a new mineral from the Bultfontein mine, Kimberley. Mineralogical Magazine (31), 607-610.
[25] Merlino, S. (1988): The structure of reyerite, $(K,Na)_2Ca_{14}Al_2Si_{22}O_{58}\cdot(OH)_8\cdot 6H_2O$. Mineralogical Magazine (52), 247-256.
[26] Dana, ES (1892): Dana's system of mineralogy, (6th ed.) apophyllite p.566-569, okenite p565, gyrolite, p.566.
[27] Dunn, PJ, Rouse, RC and Norberg, JA (1978): Hydroxyapophyllite, a new mineral, and a redefinition of the apophyllite group, 1. Description, occurrences, and nomenclature. American Mineralogist (63), 196-202.
[28] Dunn, PJ and Wilson, WE (1978): Nomenclature revisions in the apophyllite group: hydroxyl apophyllite, apophyllite, fuorapophyllite. The Mineralogical Record (9), 95-98.
[29] Gard, JA and Taylor, HFW (1956): Okenite and nekoite. Mineralogical Magazine (31), 5-20.
[30] Mackay, A and Taylor, HFW (1953): Gyrolite Mineralogical Magazine (30), 80-91
[31] Aguirre, L, Dominguez-Bella, S, Morata, D and Wittke, O (1998): An occurrence of tobermorite in Tertiary basalts from Patagonia, Chile. The Canadian Mineralogist (36), 1149-1155.
[32] Claringbull, GF and Hey, M (1952): A re-examination of tobermorite, Mineralogical Magazine (29), 960.
[33] Henmi, C and Kusachi, I (1989): Clinotobermorite, $Ca_5Si_6(O,OH)_{18}\cdot 5H_2O$, a new mineral from Fuka, Okayama Prefecture, Japan, Mineralogical Magazine (56), 353-358.
[34] Dana, ES and Ford, WE (1909): Dana's system of mineralogy (6th ed.), zeophyllite, Appendix II, p113.
[35] Parry, J, Williams, AF and Wright, FE (1932): On bultfonteinite, a new fluorine-bearing hydrous calcium silicate from South Africa. Mineralogical. Magazine (23), 145 (zeophyllite)
[36] Powder diffraction card: 00-029-1039: Reyerite, International center for diffraction data (ICDD).
[37] Kukharenko, AA, Orlova, MP, and Bulakh, AG (1965): The Caledonianultrabasic alkalic rocks and carbonatites of the Kola Peninsula and northern Karelia. Izd. Nedra,Moscow, 479-481 (in Russian).
[38] Sheppard, RA, Gude, AJ (1969): Rhodesite from Trinity County, California. American Mineralogist (54), 251-255.

TABLE 1: Compositions of Na-K-Ca-silicate hydrate minerals closely related to crystalline ASR products in concrete. From [3]

	Original formula as published		Equivalent oxide expression	Oxygen "around 20" expression	1)	2)
Crypt*	$(K,Na)_2CaSi_4O_{10}\cdot 5H_2O$	[2]	$(K,Na)_2O\cdot CaO\cdot 4SiO_2\cdot 5H_2O$	$1/2[(K,Na)_4Ca_2Si_8O_{20}\cdot 10H_2O]$	1/4	1/2
Mountainite	$KNa_2Ca_2Si_8O_{19}(OH)\cdot 6H_2O$	[17]	$Na_2O\cdot 0.5K_2O.2CaO\cdot 8SiO_2\cdot 6.5H_2O$	$Ca_2Na_2KSi_8O_{19.5}6.5H_2O$	1/4	2/3
	$NaCaK_{0.5}Si_4O_{10}3H_2O$	[18]	$1/2[Na_2O\cdot 2CaO\cdot 0.5K_2O\cdot 8SiO_2\cdot 6H_2O]$	$1/2[Na_2Ca_2KSi_8O_{19.5}6H_2O]$	1/4	2/3
	$(Ca,Na_2,K_2)_2Si_4O_{10}\cdot 3H_2O$	[18,19]	$2(Ca,Na_2,K_2)O\cdot 4SiO_2\cdot 3H_2O$	$1/2[(Ca,Na_2,K_2)_4Si_8O_{20}\cdot 6H_2O]$		
	$(Ca,Na_2,K_2)_{16}Si_{32}O_{80}\cdot 24H_2O$	[20]	$8[2(Ca,Na_2,K_2)O\cdot 4SiO_2\cdot 3H_2O]$	$4[(Ca,Na_2,K_2)_4Si_8O_{20}\cdot 6H_2O]$		
Fedorite	$KNa_4Ca_4Si_{16}O_{38}\cdot(F,Cl,OH)_2\cdot 7H_2O$	[21]	$1/2[K_2O.4Na_2O\cdot 6CaO\cdot 32SiO_2\cdot Ca_2(F,Cl,OH)_4\ 14H_2O]$	$2[K_{0.5}Na_2Ca_2Si_8O_{18.75}\cdot(F,Cl,OH)\cdot 3.5H_2O]$	1/4	4/5
	$KNa_4Ca_4(Si,Al)_{16}O_{36}(OH)_4\cdot 6H_2O$	[22]	$1/2[K_2O.4Na_2O\cdot 8CaO\cdot 32(Si,Al)O_2\cdot 16H_2O]$	$2[K_{0.5}Na_2Ca_2(Si,Al)_8O_{19}\cdot 4H_2O]$		4/5
Shly**	$(K,Na)CaSi_4O_9(OH)\cdot 3H_2O$	[2]	$1/2[(K,Na)_2O\cdot 2CaO\cdot 8SiO_2\cdot 7H_2O]$	$1/2[(K,Na)_2Ca_2Si_8O_{19}7H_2O]$	1/4	1
Rhodesite	$HKCa_2Si_8O_{19}\cdot 6H_2O$	[23]	$1/2[K_2O\cdot 4CaO\cdot 16SiO_2\cdot 13H_2O]$	$KCa_2Si_8O_{18.5}6.5H_2O$	1/4	2
	$KHCa_2Si_8O_{19}5H_2O$	[18,19]	$1/2[K_2O\cdot 4CaO\cdot 16SiO_2\cdot 11H_2O]$	$KHCa_2Si_8O_{19}5H_2O$	1/4	2
	$(Ca,Na_2,K_2)_8Si_{16}O_{40}\cdot 11H_2O$	[20]	$8(Ca,Na_2,K_2)O\cdot 16SiO_2\cdot 11H_2O$	$2[(Ca,Na_2,K_2)_4Si_8O_{20}.5.5H_2O]$		
	$4(Ca,Na_2,K_2)O\cdot 10SiO_2\cdot 7H_2O$	[24]	$4(Ca,Na_2,K_2)O\cdot 10SiO_2\cdot 7H_2O$	$(Ca,Na_2,K_2)_4Si_{10}O_{24}7H_2O$		
Reyerite	$(K,Na)_2Ca_{14}Al_2Si_{22}O_{58}\cdot(OH)_8\cdot 6H_2O$	[25]	$(K,Na)_2O\cdot 14CaO\cdot Al_2O_3\cdot 22SiO_2\cdot 10H_2O$	$3[(K,Na)_{0.67}Ca_{4.67}Al_{0.67}Si_{7.33}O_{20.67}\cdot 3.33H_2O]$	7/11	7

* cryptophyllite, ** shlykovite 1) [Ca/Si], 2) [Ca]/[Na+K]

TABLE 2: EDS compositions of rosette crystals filling cracks of coarse aggregate in concretes undergoing ASR or ACR, and in mortar bar with alkali-silicate reaction– mineral identification of possible solid solution series. Selected from [3]

	Crypto/mount*		Mountainite**				Fedorite**			Shlykovite						Shlyk/rhod***	
	Oh 2 sands ASR	Fu2 muds ASR	Oh 1 muds ASR	Ma 1 and ASR	Os 6 ls ASR	NS void ASLR	duV dol.ls ASR	Ma1 and ASR	Ms4 muds ASR	Ma 2 and ASR	duV dol.ls ASR	Ste.F dol.ls ASR	Mo dol ASR	Os 6 ls ASR	Ga dol.ls ACR	Ga dol.ls ACR	NF 108 muds ASR
SiO_2	42.40	40.85	39.59	45.33	47.87	40.64	47.20	45.29	44.16	45.23	42.51	44.83	43.79	44.79	47.68	60.13	50.72
TiO_2	0.00	0.34	0.06	0.10	0.00	0.01	0.00	0.11	0.06	0.00	0.38	0.07	0.00	0.06	0.36	0.22	0.00
Al_2O_3	0.18	0.03	0.01	0.00	0.00	0.00	0.35	0.00	0.00	0.29	0.43	0.14	0.32	0.00	2.45	0.63	0.46
FeO ****	0.34	0.31	0.32	0.50	0.16	0.08	0.08	0.00	0.00	0.04	0.00	0.00	0.23	0.15	0.00	0.08	0.13
MnO	0.32	0.00	0.49	0.51	0.09	0.04	0.09	0.00	0.00	0.00	0.32	0.08	0.01	0.24	0.00	0.00	0.00
MgO	0.00	0.00	0.00	0.00	0.00	0.00	0.00	0.00	0.00	0.00	0.00	0.00	0.00	0.00	2.06	0.00	0.00
CaO	10.52	9.85	9.27	10.63	14.97	10.40	10.95	10.77	10.21	10.98	9.00	10.74	10.59	10.48	10.07	13.55	11.39
Na_2O	3.48	3.53	2.10	2.69	2.59	6.89	2.24	2.14	2.42	0.83	1.36	0.74	0.76	1.30	5.32	0.47	4.07
K_2O	8.45	8.63	7.64	7.37	6.70	0.72	8.01	7.39	7.48	7.73	7.17	7.31	6.89	6.69	0.76	6.77	1.08
SO_3	0.00	0.34	0.00	0.03	0.06	0.00	0.00	0.00	0.00	0.08	0.00	0.00	0.00	0.12	0.34	0.00	
Total	65.69	63.88	59.92	67.16	72.44	58.78	68.92	65.70	64.33	65.19	61.17	63.95	62.58	63.83	69.04	81.85	67.85
Tetrahedral	8.04	8.01	7.91	7.98	7.84	7.93	8.00	7.96	7.96	7.97	7.94	7.97	7.99	7.94	8.01	7.95	7.94
Si	8.00	7.95	7.91	7.97	7.83	7.93	7.94.	7.96	7.96	7.90	7.84	7.94	7.92	7.98	7.51	7.85	7.85
Al	0.04	0.01	0.00	0.00	0.00	0.00	0.07	0.00	0.00	0.06	0.09	0.03	0.07	0.00	0.46	0.10	0.08
S	0.00	0.05	0.00	0.00	0.01	0.00	0.00	0.00	0.00	0.01	0.00	0.00	0.00	0.02	0.04	0.00	
Octahedral	2.00	2.00	2.00	2.00	2.00	2.00	2.00	2.00	1.98	2.00	1.88	2.00	2.00	2.00	2.00	1.93	1.91
Ca	1.90	1.90	1.86	1.84	1.97	1.98	1.98	2.00	1.97	1.99	1.78	1.98	1.97	1.93	1.48	1.90	1.89
Mg	0.00	0.00	0.00	0.00	0.00	0.00	0.00	0.00	0.00	0.00	0.00	0.00	0.00	0.00	0.48	0.00	0.00
Fe	0.05	0.05	0.05	0.07	0.02	0.01	0.01	0.00	0.00	0.01	0.00	0.00	0.03	0.02	0.00	0.01	0.02
Ti	0.00	0.05	0.01	0.01	0.00	0.00	0.00	0.00	0.01	0.00	0.05	0.01	0.00	0.01	0.04	0.02	0.00
Mn	0.05	0.00	0.08	0.08	0.01	0.01	0.01	0.00	0.00	0.00	0.05	0.01	0.00	0.04	0.00	0.00	0.00
Interlayer	3.55	3.64	2.99	2.74	2.88	2.99	2.45	2.42	2.57	2.07	2.18	1.96	1.94	2.01	2.00	1.24	1.44
Ca	0.23	0.16	0.22	0.17	0.65	0.20		0.03	0.00	0.07		0.06	0.08	0.06	0.22		
Na	1.28	1.34	0.82	0.92	0.83	2.62	0.73	0.73	0.85	0.29	0.49	0.25	0.27	0.45	1.63	0.12	1.23
K	2.04	2.14	1.95	1.66	1.40	0.18	1.72	1.66	1.72	1.72	1.69	1.65	1.59	1.51	0.15	1.13	0.21
Cation	13.59	13.64	12.90	12.72	12.72	12.92	12.46	12.46	12.51	12.04	12.00	11.93	11.93	11.96	12.02	11.12	11.07
O	20.00	20.00	19.50	19.50	19.50	19.50	19.25	19.25	19.25	19.00	19.00	19.00	19.00	19.00	19.00	18.50	18.50
Ca/Si	0.27	0.26	0.26	0.25	0.34	0.27	0.25	0.25	0.25	0.26	0.23	0.26	0.26	0.25	0.23	0.24	0.24
Ca/(Na+K)	0.64	0.56	0.75	0.78	1.18	0.78	0.80	0.85	0.77	1.02	0.82	1.07	1.11	1.01	0.95	1.52	1.54

* Cryptophyllite-mountainite, ** Substantial alkali assigned to octahedral site [3,9], ***Shlykovite-rhodesite, **** Total iron as FeO

TABLE 3: XRD analysis of ASR products in New Brunswick concretes (CuKα 6-40 °2θ) and related minerals (I/I_0>2). From [3]

T-70 A Rosette		B-90 B Rosette		P-57 C Massive		Reyeite [36]			Cryptophyllite [2]			Mountainite [17]			Shlykovite [2]			Fedorite [37]			Rhodesite [38]		
d(A)	I	d(A)	I	d(A)	I	d(A)	I	hkl	d(A)	I	hkl	d(A)	I	hkl	d(A)	I	hkl	d(A)	I	hkl	d(A)	I	hkl
12.82	27	13.12	29			19.0	40	001	16.01	100	002	13.22	15	100	13.33	100	002						
		11.72	53	11.92	86													11.7	80	001	11.8	18	020
9.752	49	9.666	100			9.5	25	002															
9.107	67					8.45	6	100															
		7.760	20	7.569	95	7.72	20	101	7.98	24	004							7.9	20	010			
6.889	34	6.976	34	6.916	98							6.702	45	102	6.67	76	004				6.73	10	111
												6.593	42	200	6.47	55	100				6.55	100	101
						6.32	8	003	6.24	48	101										6.30	30	111
				6.092	100				5.83	8	013	5.902	15	011	6.01	24	102	6.0	80	002	5.90	35	040
				5.663	95							5.647	3	111	5.65	11	102				5.73	6	121
									5.33	16	006	5.375	7	102							5.25	6	131
5.109	44	5.156	21			5.07	5	103							4.835	26	104				5.03	30	131
		4.719	22			4.88	3	110	4.752	14	110	4.697	23	112	4.717	22	111				4.80	12	002
						4.73	7	111	4.651	16	111	4.663	18	210	4.552	2	112	4.67	30	130			
4.419	42					4.34	14	112	4.338	18	105				4.447	17	104	4.38	10	200	4.39	45	220
4.283	45	4.235	35			4.23	60	200	4.229	3	113				4.290	9	113	4.21	70	113			
				4.117	72	4.14	8	104				4.161	12	112	4.113	24	113				4.10	10	221
3.923	52					3.858	30	202	3.918	2	107				3.978	36	114	4.00	60	112	3.94	4	122
		3.882	32	3.878	69	3.800	10	005										3.85	20	041	3.83	8	231
3.727	49	3.752	43						3.716	5	115	3.764	8	113	3.790	27	114	3.78	10	220	3.72	6	240
3.596	72	3.654	71	3.597	72				3.656	9	116	3.672	8	013				3.65	10	201			
		3.539	47			3.514	45	203							3.529	37	106	3.56	20	223			
3.431	100	3.442	50	3.435	62	3.467	10	105	3.484	14	021	3.346	11	311	3.469	45	021				3.38	20	250
3.310	73	3.291	34									3.300	13	400	3.337	20	008	3.35	40	133	3.27	8	202
				3.214	65				3.228	22	109				3.215	13	202	3.24	10	132	3.24	16	152
		3.189	33			3.191	9	210	3.197	27	0.0.10	3.198	21	120									
						3.150	100	211	3.163	9	019	3.156	3	121	3.143	2	116						
									3.121	15	202				3.084	11	202	3.13	80	113			
3.060	78	3.068	36						3.068	17	025				3.068	57	121				3.07	20	113
				3.044	65	3.029	40	212	3.043	8	122	3.038	27	411	3.042	45	121	3.04	40	242	3.02	20	242
3.003	58					2.996	10	115	2.995	47	122	2.988	23	214	2.996	32	204	2.97	90	151	3.00	20	123
		2.964	75			2.963	6	106	2.938	16	119	2.961	100	014	2.945	62	123				2.955	16	162
2.926	63			2.928	63				2.903	84	124	2.944	33	213	2.912	90	212	2.93	100	224	2.947	12	301
									2.877	18	213				2.877	24	123				2.887	16	133
2.845	38	2.852	47			2.849	90	213	2.843	16	212	2.810	15	122	2.830	17	212				2.864	25	331
				2.774	46	2.817	10	300	2.765	3	027	2.791	18	314	2.756	10	026	2.80	40	241	2.778	6	270
2.723	57					2.708	8	007	2.709	8	126				2.718	12	125	2.74	20	331	2.762	25	331
2.636	30					2.650	60	116	2.623	20	126	2.641	5		2.654	5	118				2.744	12	143
															2.623	7	125	2.67	30	061	2.692	4	271
									2.578	3	1.0.11	2.604	8	223	2.573	12	126	2.60	60	115	2.624	4	262
		2.526	19									2.518	1	512	2.540	10	216				2.518	6	223
2.498	51			2.469	24				2.479	6	0.1.12	2.451	1	510	2.494	5	0.1.10				2.513	6	22x
2.415	33	2.440	21			2.440	16	215				2.410	2	504	2.438	7	127	2.42	40	135	2.461	4	191
2.380	48	2.380	22						2.394	6	1.1.11	2.382	4	124				2.36	30	044	2.434	4	182
2.346	45								2.349	14	219	2.348	3	420	2.318	3	223	2.32	10	352			
2.287	30											2.317	5	115									

TABLE 4: Compositions of Canadian phyllosilicates undergoing "alkali-silicate reaction" as compared with Japanese sample. Single measurements. From [3]

	Accelerated mortar bar (Nova Scotia aggregate)							Field concrete (Japan)		
	Biotite		Muscovite			Chlorite		Biotite	Muscovite	
	Sandstone boundary	Sandstone interior	Sandstone boundary	Sandstone near crack	Mudstone near gel	Sandstone boundary	Mudstone near gel	Mudstone in gel	Mudstone in gel	Mudstone in gel
SiO_2	36.53	36.35	45.92	45.86	47.76	25.21	25.09	33.91	43.62	45.69
TiO_2	1.41	1.10	0.17	0.43	0.37	0.00	0.29	2.51	0.98	0.46
Al_2O_3	17.02	16.20	27.65	28.06	29.31	19.38	18.22	16.56	28.15	24.85
FeO*	21.91	22.62	2.68	3.23	2.68	31.05	28.53	21.87	1.50	2.18
MnO	0.00	0.00	0.23	0.19	0.00	0.11	0.00	0.14	0.56	0.41
MgO	7.96	8.08	0.86	0.62	0.76	10.82	9.62	8.15	0.40	1.45
CaO	0.02	0.00	0.30	0.00	0.21	0.65	0.79	0.00	0.14	0.00
Na_2O	0.27	0.29	0.47	0.18	0.17	0.48	0.45	0.17	0.36	0.36
K_2O	9.33	8.62	10.58	10.97	11.00	0.11	0.35	9.72	10.41	11.24
SO_3	0.37	0.31	0.00	0.00	0.00	0.05	0.00	0.21	0.29	0.00
Total	94.82	93.57	88.86	89.54	92.26	87.86	83.34	93.24	86.41	86.64
Tetrahedral	8.00	8.00	8.00	8.00	8.00	4.00	4.00	8.00	8.00	8.00
Si	5.54	5.61	6.61	6.55	6.58	2.75	2.85	5.24	6.38	6.75
Al	2.42	2.35	1.39	1.42	1.46	1.25	1.15	2.74	1.59	1.25
S	0.04	0.04	0.00	0.00	0.00	0.00	0.00	0.02	0.03	0.00
Octahedral	5.38	5.52	3.86	3.87	3.86	3.00	3.00	5.30	3.72	3.77
Al	0.63	0.60	3.31	3.28	3.36	1.24	1.29	0.28	3.27	3.08
Ti	0.16	0.13	0.02	0.06	0.04	0.00	0.02	0.29	0.11	0.05
Mg	1.80	1.86	0.18	0.13	0.16	0.67	1.63	1.88	0.09	0.32
Fe	2.79	2.93	0.32	0.39	0.31	1.08	2.72	2.83	0.18	0.27
Mn	0.00	0.00	0.03	0.02	0.00	0.01	0.00	0.02	0.07	0.05
Interlayer	1.89	1.79	2.12	2.05	2.01	3.04	2.91	1.97	2.07	2.22
Ca	0.00	0.00	0.05	0.00	0.03	0.08	0.10	0.00	0.02	0.00
Na	0.08	0.09	0.13	0.05	0.05	0.10	0.10	0.05	0.10	0.10
K	1.81	1.70	1.94	2.00	1.94	0.02	0.05	1.92	1.94	2.12
Mg						1.09	1.00			
Fe						1.76	1.66			
Cation	15.28	15.31	13.99	13.92	13.88	10.04	9.91	15.28	13.79	14.00
O	22.00	22.00	22.00	22.00	22.00	14.00	14.00	22.00	22.00	22.00
Fe/(Mg+Fe)	0.61	0.61	0.64	0.75	0.66	0.62	0.62	0.60	0.68	0.46

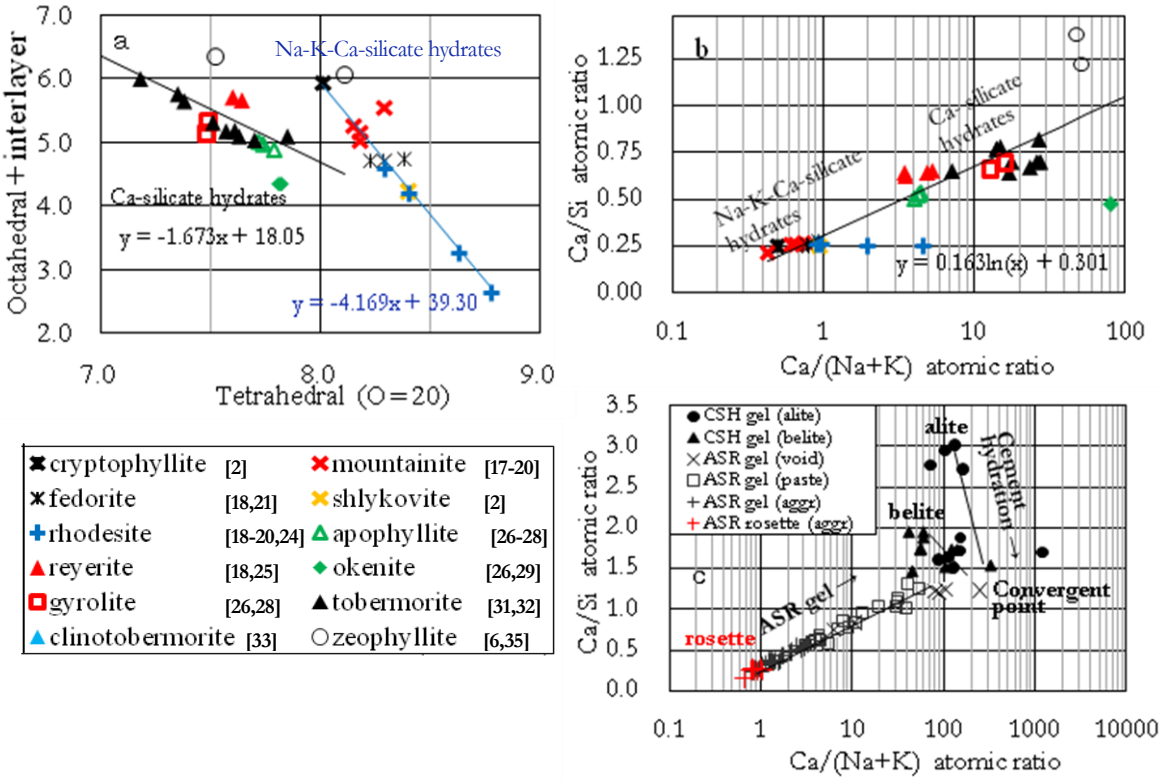

FIGURE 1: Na-K-Ca-silicate hydrate and Ca-silicate hydrate minerals, plotted for a) cation distributions, and b) cation ratios on [Ca/Si]-[Ca]/[Na+K] diagram. c) cation ratios of ASR products and calcium silicate hydrates (cement hydrates) from alite and belite in less weathered concrete (Ma, Japan), plotted on [Ca/Si]-[Ca]/[Na+K] diagram (Ma). Modified from [3]

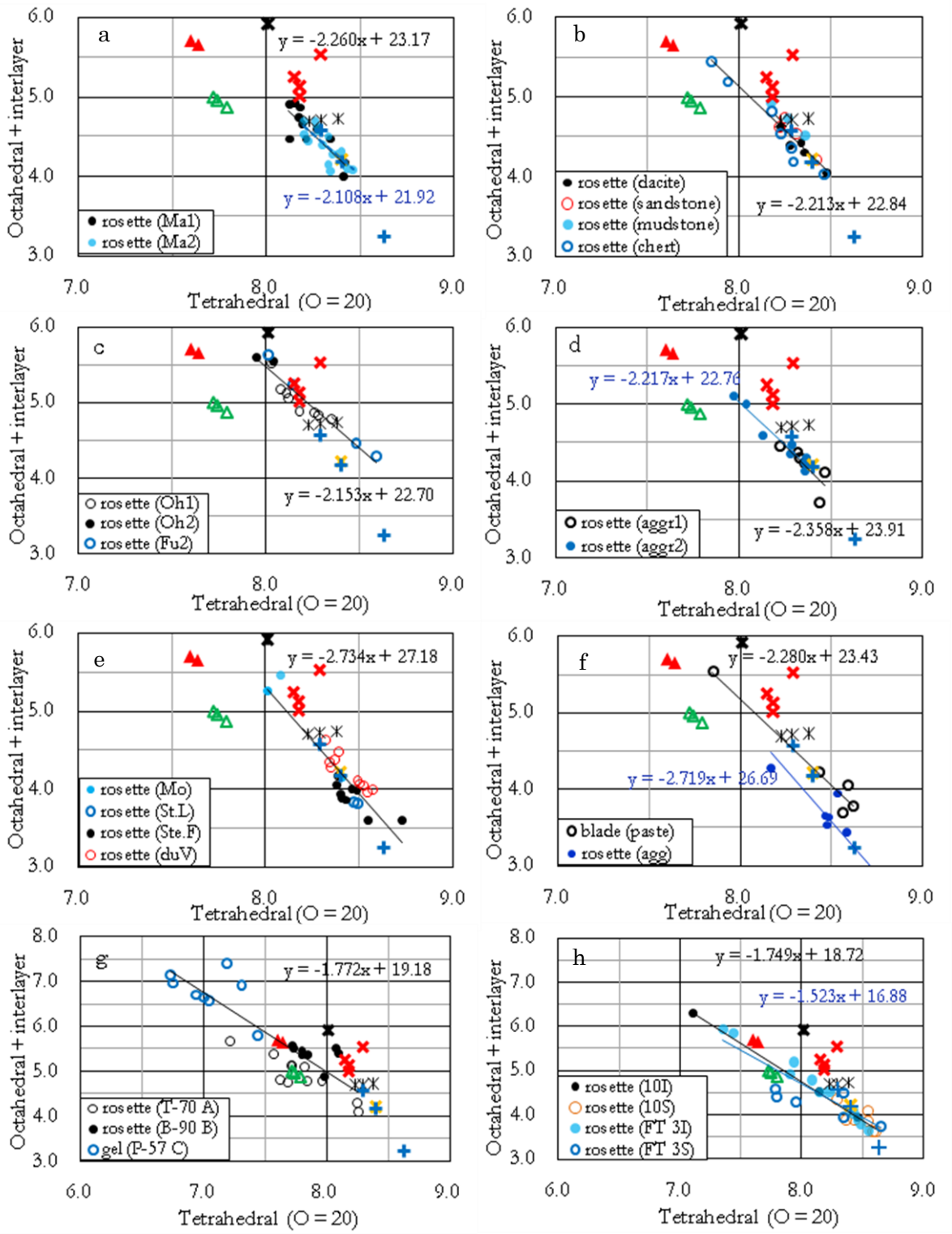

FIGURE 2: Cation sites of crystalline ASR products: a) andesite (Ma, Japan), b) sedimentary rocks (Mi, Japan), c) sandstone and mudstone (Oh, Fu, Japan). d) limestone (Os, Norway), e) dolomitic limestone (Mo, St.L, Ste.F, duV, Quebec). f) ACR of dolomitic limestone (Ga, Ontario); sandstone and mudstone in g) field concretes (Tr, Br, Pi, New Brunswick) and in h) concrete prisms (with/without freeze-thaw, Newfoundland). Legends refer to Figure 1. Modified from [3]

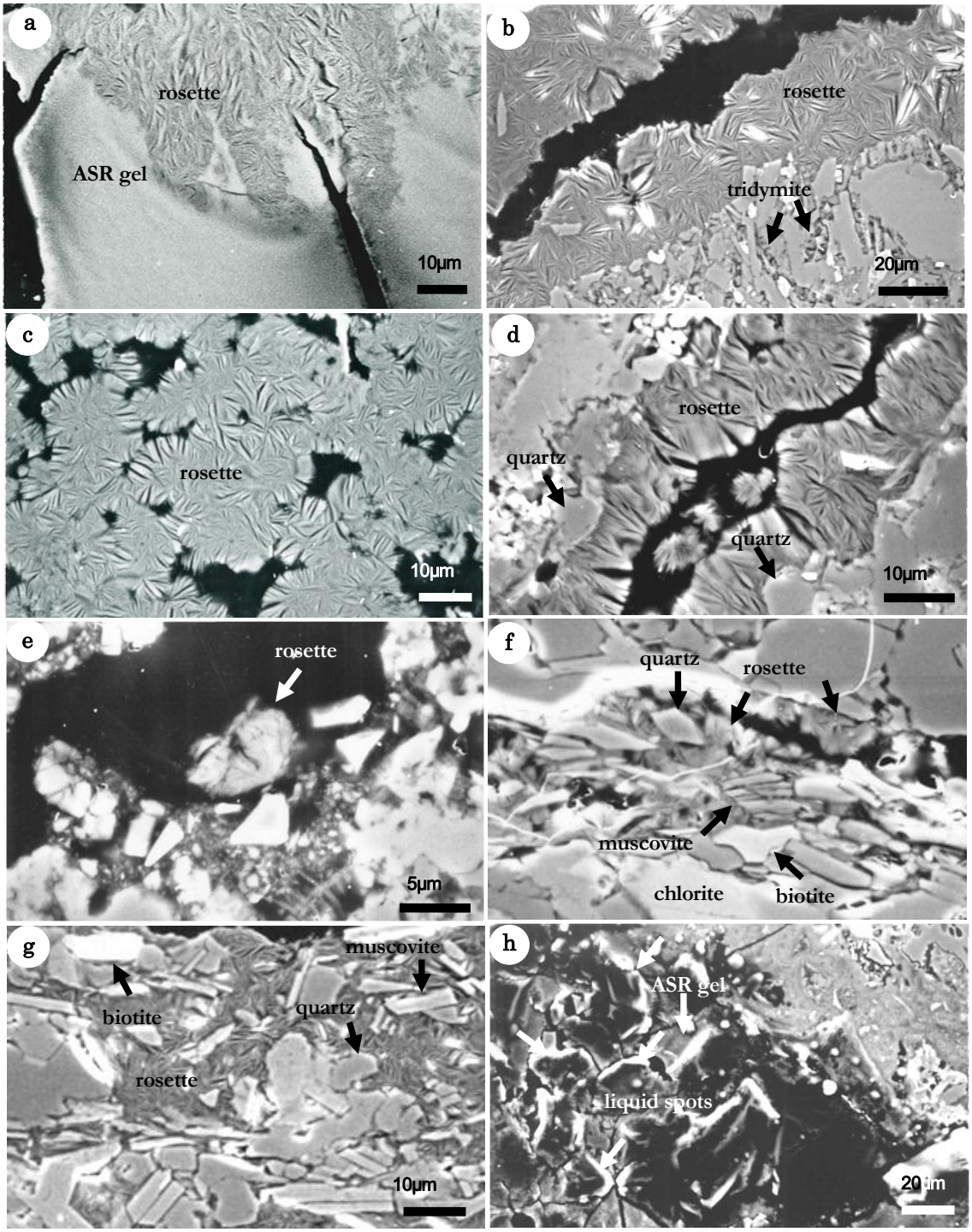

FIGURE 3: Rosettes crystallized from ASR gel filling cracks of aggregate: a) cryptophyllite-mountainite crystallizing from ASR gel (sandstone, Oh2, Japan [8]), b) mountainite (andesite, Ma1, Japan), c) shlykovite (dolomitic limestone, duV, Quebec), d) shlykovite (limestone, Os, Norway). e) rhodesite in *alkali-carbonate reaction* (dolomitic limestone, Ga, Ontario), f) ASR rosettes enclosing unreacted phyllosilicate flakes and reacted microcrystalline quartz in "alkali-silicate reaction" (sandstone, Nova Scotia: mortar bar), g) Vein of ASR rosettes enclosing unreacted phyllosilicates (mudstone hornfels, Hy, Japan). h) Separated liquid spots (dark) from ASR gel under carbon coating on polished thin section (glassy rhyolite, To, Japan). Modified from [3]

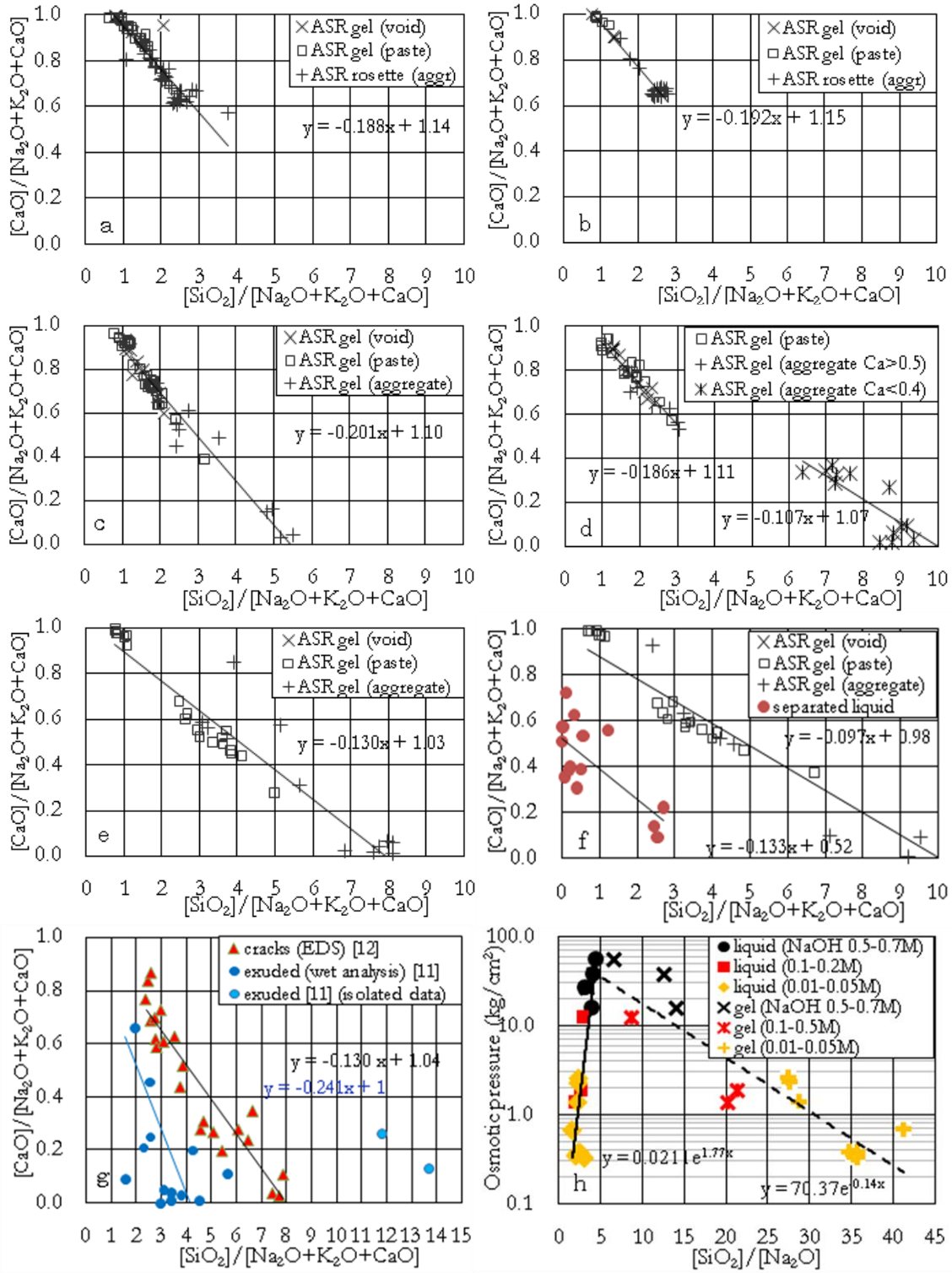

FIGURE 4: Spontaneous separation of alkali-rich silica sol from ASR gel, leaving silica-rich ASR gel: Rosette, a) before and b) after cleaning up the blots of sol 1 year later (Ma); ASR gel, c) before and d) after cleaning up sol 9 years later (Ji); ASR gel, e) original and f) 1 year later without cleaning up the separated sol (To). g) comparison between fluid and viscose gel in ASR concretes recalculated from [11,12], h) Equilibrated pair of alkali-silica sol and silica gel redrawn from [13]. Modified from [3]

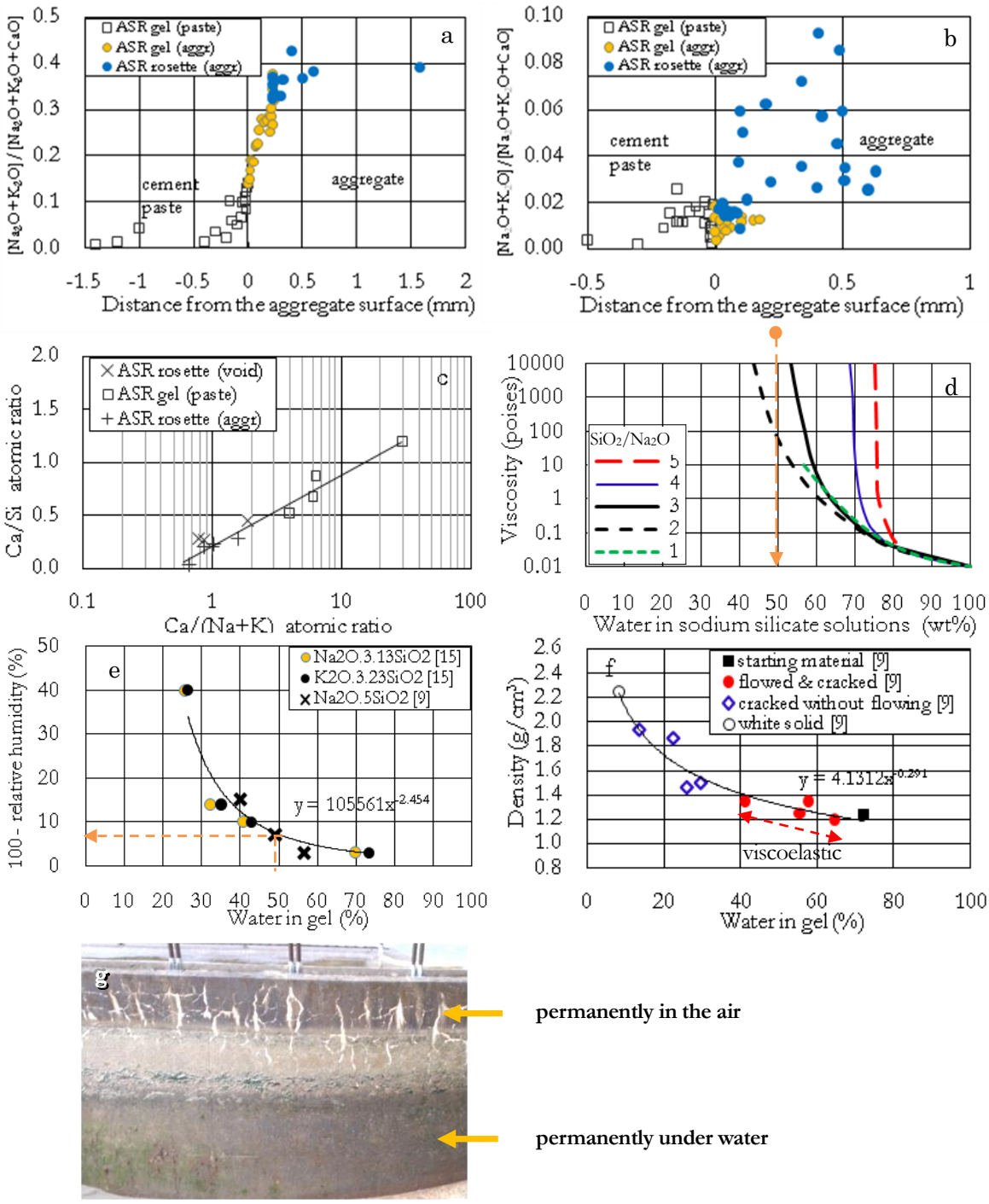

FIGURE 5: Compositions of ASR gel vein within single crack of aggregate particle in a) less weathered concrete (Ma, same as in Figs.1c,2a,3b,4a: andesite, Japan), and in b) highly weathered concrete showing the leaching of alkalis (NF, Newfoundland, Canada: sandstone). c) [Ca/Si]-[Ca]/[Na+K] diagram for ASR products of "alkali-silicate reaction" in accelerated mortar bar (NS, Nova Scotia, Canada: greywacke), d) viscosity of alkali-silica sol, re-calculated and extrapolated from [14], e) relative humidity vs. water content of alkali-silica gel, modified from [9,15], f) density vs. water content of gel, modified from Vivian [9]; a)-f) from [3]; g) absence of ASR gel and cracks on the concrete surface in contact with flowing water (inner wall, canal, Japan: andesite) due to dissolution of ASR sol, while dried portion develops cracking.